Infection, Genetics and Evolution 116 (2023) 105516

Contents lists available at ScienceDirect

Infection, Genetics and Evolution

journal homepage: www.elsevier.com/locate/meegid

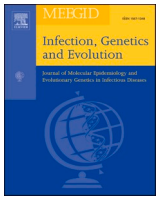

In silico prediction of interaction between Nipah virus attachment glycoprotein and host cell receptors Ephrin-B2 and Ephrin-B3 in domestic and peridomestic mammals

Ananya Ferdous Hoque [a,1], Md. Mahfuzur Rahman [a,e,1], Ayeasha Siddika Lamia [a], Ariful Islam [b], John D. Klena [c], Syed Moinuddin Satter [a], Jonathan H. Epstein [b], Joel M. Montgomery [c], Mohammad Enayet Hossain [a], Tahmina Shirin [d], Iqbal Kabir Jahid [e], Mohammed Ziaur Rahman [a,*]

[a] *Infectious Diseases Division (IDD), icddr,b, 68, Shaheed Tajuddin Ahmed Sarani, Mohakhali, Dhaka 1212, Bangladesh*
[b] *EcoHealth Alliance, 520 8th Ave Ste. 1200, New York, NY 10018, USA*
[c] *Viral Special Pathogens Branch, Centers for Disease Control and Prevention, 1600 Clifton Rd. NE, Atlanta, GA 30333, USA*
[d] *Institute of Epidemiology, Disease Control and Research (IEDCR), Mohakhali, Dhaka 1212, Bangladesh*
[e] *Department of Microbiology, Jashore University of Science and Technology, Jashore 7408, Bangladesh*

ARTICLE INFO

Keywords:
Molecular docking
Protein-protein interaction
Nipah virus
Glycoprotein
Ephrin

ABSTRACT

Nipah virus (NiV) is a lethal bat-borne zoonotic virus that causes mild to acute respiratory distress and neurological manifestations in humans with a high mortality rate. NiV transmission to humans occurs *via* consumption of bat-contaminated fruit and date palm sap (DPS), or through direct contact with infected individuals and livestock. Since NiV outbreaks were first reported in pigs from Malaysia and Singapore, non-neutralizing antibodies against NiV attachment Glycoprotein (G) have also been detected in a few domestic mammals. NiV infection is initiated after NiV G binds to the host cell receptors Ephrin-B2 and Ephrin-B3. In this study, we assessed the degree of NiV host tropism in domestic and peridomestic mammals commonly found in Bangladesh that may be crucial in the transmission of NiV by serving as intermediate hosts. We carried out a protein-protein docking analysis of NiV G complexes ($n = 52$) with Ephrin-B2 and B3 of 13 domestic and peridomestic species using bioinformatics tools. Protein models were generated by homology modelling and the structures were validated for model quality. The different protein-protein complexes in this study were stable, and their binding affinity (ΔG) scores ranged between −8.0 to −19.1 kcal/mol. NiV Bangladesh (NiV-B) strain displayed stronger binding to Ephrin receptors, especially with Ephrin-B3 than the NiV Malaysia (NiV-M) strain, correlating with the observed higher pathogenicity of NiV-B strains. From the docking result, we found that Ephrin receptors of domestic rat (*R. norvegicus*) had a higher binding affinity for NiV G, suggesting greater susceptibility to NiV infections compared to other study species. Investigations for NiV exposure to domestic/peridomestic animals will help us knowing more the possible role of rats and other animals as intermediate hosts of NiV and would improve future NiV outbreak control and prevention in humans and domestic animals.

1. Introduction

Nipah virus (NiV) is an emerging pathogen that causes encephalitis and acute respiratory distress in humans (Bellini et al., 2005; WHO, 2018). NiV has zoonotic origins and fruit bats commonly referred to as "flying foxes" from the *Pteropus* genus are its natural host and reservoir (Aditi and Shariff, 2019; Skowron et al., 2022). In Bangladesh, the case fatality rate of NiV infections varies between 70 and 100% and is linked to the consumption of raw date palm sap (DPS) contaminated with infected bat saliva or excreta (Nikolay et al., 2019; Luby et al., 2006). No

* Corresponding author at: Senior Scientist & Head, One Health Laboratory, Infectious Diseases Division, icddr,b, 68, Shaheed Tajuddin Ahmed Sarani, Mohakhali, Dhaka 1212, Bangladesh.
E-mail address: mzrahman@icddrb.org (M.Z. Rahman).
[1] Both authors contributed equally to this manuscript.

https://doi.org/10.1016/j.meegid.2023.105516
Received 5 July 2023; Received in revised form 11 September 2023; Accepted 18 October 2023
Available online 2 November 2023

specialized vaccines or therapeutic drugs are available for NiV infections, making it a priority zoonotic illness requiring immediate research attention (Banerjee et al., 2019; WHO, 2018). The Centers for Disease Control and Prevention (CDC), USA, have designated NiV as a Biosafety Level-4 agent (Bioterrorism Agents/Diseases, 2023; Biosafety in Microbiological and Biomedical Laboratories (BMBL) 6th Edition, 2020). The first reported outbreak of human NiV infections was in the Malaysia-Singapore region, in 1998–1999, where the majority of human infections were caused due to direct exposure to diseased pigs (Bellini et al., 2005; Paton et al., 1999; Outbreak of Hendra-like virus–Malaysia and Singapore, 1998–1999, 1999). NiV infection is endemic in parts of Asia like Bangladesh and India, where outbreaks occur annually in seasonal patterns (Aditi and Shariff, 2019; Soman Pillai et al., 2020). In Bangladesh, the first case of NiV was reported in 2001 (Aditi and Shariff, 2019; Nikolay et al., 2019). Until now, two separate strains of NiV, Malaysia (NiV-M) and Bangladesh (NiV-B) have been isolated. NiV-B and NiV-M strains are 91.8% similar at the nucleotide level, although NiV-B displays greater intra-strain genetic variability (Clayton et al., 2012; Hauser et al., 2021). Despite sharing a high percentage of homology, NiV-B causes increased incidences of respiratory disease and oral shedding in patients than NiV-M (Clayton et al., 2012). NiV-B infections show diverse transmission patterns and higher fatality rates compared to NiV-M, hence it is considered to be more pathogenic (Soman Pillai et al., 2020; Mire et al., 2016).

NiV is a member of the *Paramyxoviridae* family and *Henipavirus* genus, characterized as an enveloped virus. NiV contains a negative-sense single-stranded RNA genome encoding six main structural proteins. The attachment glycoprotein (G) of NiV is classified as a type II membrane protein and it plays a vital role in viral attachment to the host cell (Xu et al., 2008; Bowden et al., 2008a). The NiV-G has a tetramer structure, however, only one of the ectodomain homotetramers is engaged in receptor binding (Wang et al., 2022). The NiV-G recognizes and binds to host cell Ephrin-B2 and B3 receptors. Ephrin molecules are receptor tyrosine kinases involved in cell signalling, hence they are broadly expressed and are highly conserved across vertebrates (Xu et al., 2008; Bowden et al., 2008a). The NiV G ectodomain homotetramer contains a six-bladed β propeller domain that forms a 1:1 protein-protein interface with the protruding G-H loop of Ephrin-B2 and B3 (Xu et al., 2008; Bowden et al., 2008a; Wang et al., 2022). Upon binding, the NiV-G undergoes conformational changes facilitating the fusion (F) glycoprotein-mediated viral fusion with the host cell membrane to initiate infection. NiV-G is a favourable target for neutralizing antibodies as well as drug design (Bhuiyan et al., 2022).

NiV disease is a “One Health” concern, exhibiting a broad species tropism and causes diseases in animals and humans (WHO, 2018; Aditi and Shariff, 2019). Bat-to-human transmission of NiV can occur directly or through an intermediate host such as pigs (Skowron et al., 2022). In Malaysia, NiV infections were serologically detected in dogs, but there was no evidence of virus transmission within the dog population in the absence of infected pigs (Mills et al., 2009). Antibodies against NiV-G have been detected by a Luminex-based multiplexed assay, but all were negative in ELISA and serum neutralization assays among Bangladeshi domestic animals (pigs, cattle, and goats). This could be due to potential exposure to other henipaviruses or henipa-like viruses that exhibit antigenic resemblance to NiV (Chowdhury et al., 2014). NiV has not been found in wild rodents, though a related set of henipavirus-like Paramyxoviruses, including Mojiang virus, have been found in rats (*e.g. Ratus flavivpectus*) (Drexler et al., 2012; Wu et al., 2014). Mojiang virus, however, does not use the Ephrin-B2 receptor - its receptor remains unknown (Cheliout Da Silva et al., 2021). Rodents have variable susceptibility to NiV. Experimental studies of animal models have found that mice have limited susceptibility to NiV while golden hamsters (*Mesocricetus auratus*) are highly susceptible and have been used as a model for human disease (de Wit and Munster, 2015; Wong et al., 2003). Data supporting host susceptibility to NiV are mostly based on epidemiological and serological studies. Some animal experiments have been performed to understand host susceptibility, but these have generally been limited to traditional lab animal models rather than peridomestic wildlife species (Weingartl et al., 2009). An *in vitro* study has shown that NiV is capable of infecting cells that express soluble Ephrin-B2 and B3 ligands cloned from a range of species (human, bat, pig, horse, cat, dog, and mouse) without any notable variations in receptor function between the species. The research further demonstrates the inhibition of NiV infections, through the use of ephrin ligands and human monoclonal antibodies specific to NiV G. (Bossart, 2007). A better understanding of how NiV G interacts with host cell receptors Ephrin-B2 and B3 in domestic and peridomestic mammals is required as it plays a vital role in infection. With the expanding advancements in bioinformatics, *in silico* prediction approach has become a powerful tool to model host-pathogen interaction through docking in the post-genomic era. Here, we conducted a protein-protein docking analysis of NiV G with the Ephrin-B2 and B3 receptors from domestic and peridomestic mammals to evaluate their potential as susceptible or intermediate hosts for NiV infections. Our results show molecular evidence of the relative susceptibility of domestic and peridomestic mammals to NiV infections which will provide knowledge and information to control and prevent future outbreaks.

2. Methods and materials

2.1. Data mining

Two complete amino acid sequences of NiV attachment Glycoprotein (G) (602 residues) belonging to NiV-B and M strains were retrieved from the National Center for Biotechnology Information (NCBI) (https://www.ncbi.nlm.nih.gov/protein) database (Table S1). Considering the limited diversity between the reported NiV-B and NiV-M strains, the reference sequences used in previous evolutionary studies were selected as representatives for our prediction analysis (Whitmer et al., 2020; Harcourt et al., 2005). The amino acid sequences of Ephrin-B2 (333 residues) and Ephrin-B3 (340 residues) proteins were retrieved for previously reported hosts and reservoirs of NiV like a human (*Homo sapiens*), bat (Indian flying fox *Pteropus medius* (formerly *P. giganteus*) (Mlikovsky, 2012)) and pig (*Sus scrofa*) along with other domestic and peridomestic mammals commonly found in Bangladesh. The domestic host group included cattle (*Bos tarus and B. indicus*), buffalo (*Bubalus bubalis*), sheep (*Ovis aries*), goat (*Capra hircus*), donkey (*Equus asinus*), horse (*Equus caballus*), dog (*Canis lupus familiaris*) and cat (*Felis catus*). The peridomestic host group consisted of mouse (*Mus musculus*) and rat (*R. norvegicus*) (Table S1).

2.2. Protein sequence analyses

Orthologues of host cell receptors Ephrin-B2 and B3 are expressed in many cells and tissues of mammalian species. MEGA-X (version 10.0.5) software was used to evaluate the amino acid dissimilarity among Ephrin-B2 and B3 receptors from the domestic and peridomestic study species compared to human cellular receptors (Ephrin-B2_EAX09085.1 and Ephrin-B3_KAI4047722.1). The *p*-distance matrix was calculated by comparison to the human sequences using a Jones-Taylor-Thornton (JTT) model (Whelan and Goldman, 2001). The phylogenetic analyses were performed with amino acid sequences of Ephrin-B2 and B3 from study species using MEGA-X (version 10.0.5) software. The phylogenetic tree was created with 1000 bootstrap replications using the Maximum Likelihood method and JTT matrix-based model. Multiple amino acid alignments of Ephrin-B2 and B3 protein sequences were done using the ClustalW multiple alignments feature in BioEdit v7.2 software. Jalview (Version: 2.11.2.4) software was used for the visualization and analysis of Ephrin-B2 and B3 binding residues at the protein-protein interface with NiV G (Waterhouse et al., 2009).

2.3. Protein preparation

The crystal structure data of NiV-G (PDB ID: 2VWD), Ephrin-B2 (PDB ID: 1IKO), NiV-G complex with human Ephrin-B2 (PDB ID: 2VSM) and mouse Ephrin-B3 (PDB ID: 3D12) was retrieved from RCSB Protein Data Bank (https://www.rcsb.org/) (Xu et al., 2008; Bowden et al., 2008a; Bowden et al., 2008b; Berman et al., 2000; Toth et al., 2001). AutoDock Tools (version 1.5.7) software package was used to add missing hydrogens and remove ions, water molecules, and ligands from the structures. These structures were used as a reference to validate the quality of homology-modelled complexes.

2.4. Homology modelling

Homology structural modelling was performed to predict the structural conformation of all NiV G, Ephrin-B2, and B3 proteins (Table S1) as their experimentally determined 3D structures are unreported to date. Protein FASTA sequences retrieved from the NCBI database were used to prepare reliable models in the PHYRE2 server (http://www.sbg.bio.ic.ac.uk/~phyre2/html/page.cgi?id=index) (Kelley et al., 2015). In PHYRE2, top models were obtained from sequence alignment with template protein structures that are available across genomes followed by one-to-one threading.

2.5. Homology model validation

To check if the predicted models met the quality requirements for homology with NiV G, Ephrin-B2 and B3 template structures, models were evaluated through protein structure analysis. Ramachandran plots were generated using PROCHECK (https://www.ebi.ac.uk/thornton-srv/software/PROCHECK/) to validate the geometry and stereochemical properties of models. ProSA-web (https://prosa.services.came.sbg.ac.at/prosa.php) was used to calculate the *Z*-score which indicates overall model quality and quantifies the deviation of the model's total energy from the energy distribution of experimentally resolved PDB protein structures of similar size (Wiederstein and Sippl, 2007). The homology models of NiV G, Ephrin-B2 and B3 were structurally aligned with template structures (PDB ID: 2VWD, 1IKO, and 3D12 respectively) to measure the degree of similarity between the protein structures. The TM-Align (https://zhanggroup.org/TM-align/) algorithm was used to generate the template modelling (TM) and root-mean-square deviation (RMSD) values (Zhang and Skolnick, 2005). A TM score between 0.5 and 1.0 indicates that the protein structures are in the same fold, where 1.0 indicates a perfect match and scores below 0.2 indicate random structural similarity. Lower RMSD values indicate higher accuracy of docking and values <1 Angstrom is preferable.

2.6. Protein-protein molecular docking

In our study, a total of 52 complexes were examined using the ClusPro webserver (https://cluspro.bu.edu/login.php) to determine the binding interactions between NiV G and the host cell receptors Ephrin-B2 and B3 (Kozakov et al., 2017). Docking models were screened using a balance of electrostatic and hydrophobic scoring schemes. The near-native conformation was identified as the model with the lowest energy for each set of interacting proteins. The protein-protein interaction was analysed using the PRODIGY webserver (https://nestor.science.uu.nl/prodigy/). The PRODIGY webserver was employed to predict the binding affinity ΔG (kcal/mol) of protein-protein complexes, where greater negative values represent higher binding affinity and stability of a given complex. The dissociation constant (Kd), defined as the concentration of ligand (Ephrin-B2 or B3) at which half the ligand binding sites on the protein (NiV-G) are occupied in the system equilibrium, was also determined at body temperature 37 °C (Xue et al., 2016). PyMOL was used for all docked complexes' visualization and molecular interaction analysis.

2.7. Molecular dynamics simulation

The iMOD server (https://imods.iqfr.csic.es/) was used to perform a molecular dynamics simulation to assess the stability and physical movements of the protein-protein complexes between NiV G and mammalian cell receptors Ephrin-B2 and B3. The iMOD server generates simulation graphs that show the main-chain deformability, B-factor values, eigenvalue, variance, co-variance map and elastic network model.

3. Results

3.1. Analysis of Ephrin-B2 and B3 protein sequences

A *p*-distance matrix was calculated to study the Ephrin-B2 and B3 variability among bat (Indian flying fox), cattle, buffalo, dog, goat, donkey, horse, sheep, pig, cat, mouse and rat in comparison to human reference sequences (Fig. 2). The highest difference among Ephrin-B2 proteins was 5.4% between mouse and bat. The buffalo and cattle Ephrin-B2 proteins were homologous with 100% identity, same as horse and donkey. In the Ephrin-B3 alignment, mouse and rat had the highest difference of 6.3% with pig Ephrin-B3, whereas, identical Ephrin-B3 sequences were found between goat, buffalo, and sheep; cat and dog; and rat and mouse. The trends in amino acid sequence variability were similar to the phylogenetic relatedness found between Ephrin-B2 and B3 of the study species (Fig. 2).

3.2. Homology modelling and structure validation

Homology models for NiV-G (B and M strains) and host cell receptors Ephrin-B2 and B3 from human, bat, cattle, buffalo, dog, goat, donkey, horse, sheep, pig, cats, mouse and rat were built using template structures. All models had ≥80% of the amino acids in favourable regions for rotations and folding (Table 1). The two NiV-G models were found within the distribution of X-ray crystallography protein structures, whereas Ephrin-B2 and B3 models were validated against protein structures from NMR sources. All models displayed low RMSD scores and the TM scores were over 0.99, this indicates near-perfect matches with template structures. In general, our predicted models satisfied the quality requirements for homology with the template structures.

3.3. Prediction of NiV G interaction with Ephrin-B2 and B3

The molecular dynamic simulation results suggest that the homology docked protein-protein complexes in this study were stable (Fig. S1 and S2). The binding affinity values of all complexes ($n = 52$) calculated by the PRODIGY web server were distributed between −8.0 and − 19.1 kcal/mol (Fig. 3 and Table 2). NiV-B complexes (complexes 1 to 26) had a higher binding affinity with both Ephrin-B2 and B3 in comparison with NiV-M complexes (complexes 27 to 52) in the majority of the hosts, except for rat (ΔG of complex 39 was more negative than complex 13). In the rat group, the binding affinity (complexes 13, 39, and 51) was high compared to the energy scores calculated for the other study species including natural NiV reservoirs and hosts human, bat, and pig. NiV-B complexes with Ephrin-B3 (complexes 14 to 26) displayed strong binding as their binding affinity scores were the most negative (ΔG −18.4 to −19.1 kcal/mol) with the smallest dissociation constant values (Kd 3.40 to 9.80E-14) among all study complexes.

The binding affinity of homology docked protein-protein complexes was compared with experimentally solved complexes available on PDB. Study complexes 27 (ΔG −10.7 kcal/mol, Kd 2.90E-08) and 51 (ΔG −12.6 kcal/mol, Kd 1.20E-09) corresponded to PDB structures 2VSM and 3D12 respectively, and their binding energy scores were similar. PRODIGY predicted a binding affinity (ΔG) of −12 kcal/mol and dissociation constant (Kd) of 3.60E-09 (at 37 °C) for 2VSM. For 3D12, binding affinity (ΔG) was −12 kcal/mol and dissociation constant (Kd)

Table 1
Validation data for predicted homology models of NiV attachment Glycoprotein and host cell receptors Ephrin-B2 and B3.

Protein	Model	Model Length	Template Length	Aligned Residues	Favourable region (%)	RMSD value	TM value	Z value
Glycoprotein	NiV-BD	416	413	413	84.7	0.14	0.99	−8.36
	NiV-M	416	413	227	86.4	0.12	0.99	−8.03
Ephrin-B2	Human	141	141	141	87.7	0	1	−5.28
	Bat	141	141	141	87.7	0	1	−5.29
	Cattle	141	141	141	87.7	0	1	−5.31
	Buffalo	141	141	141	87.7	0	1	−5.31
	Dog	141	141	141	87.7	0	1	−5.31
	Goat	141	141	141	87.7	0	1	−5.31
	Donkey	141	141	141	87.7	0	1	−5.31
	Horse	141	141	141	87.7	0	1	−5.31
	Sheep	141	141	141	87.7	0	1	−5.31
	Pig	141	141	141	87.7	0	1	−5.31
	Cat	141	141	141	87.7	0	1	−5.27
	Mouse	141	141	141	87.7	0	1	−5.31
	Rat	141	141	141	87.7	0	1	−5.27
Ephrin-B3	Human	141	101	101	79.6	0.32	0.99	−3.83
	Bat	141	101	101	79.6	0.32	0.99	−3.83
	Cattle	141	101	101	79.6	0.32	0.99	−3.83
	Buffalo	141	101	101	79.6	0.32	0.99	−3.83
	Dog	141	101	101	79.6	0.32	0.99	−3.83
	Goat	141	101	101	79.6	0.32	0.99	−3.83
	Donkey	141	101	101	79.8	0.32	0.99	−4.22
	Horse	141	101	101	79.6	0.32	0.99	−3.83
	Sheep	141	101	101	79.6	0.32	0.99	−3.83
	Pig	141	101	101	79.6	0.32	0.99	−3.83
	Cat	141	101	101	79.6	0.32	0.99	−3.72
	Mouse	141	101	101	79.8	0.32	0.99	−3.83
	Rat	141	101	101	79.8	0.32	0.99	−3.83

Table 2
Summary of protein-protein docking results of NiV G complexes with host cell receptors Ephrin-B2 and B3 using ClusPro and PRODIGY webservers.

		NiV-B					NiV-M				
		Complex No.	Lowest Energy	Cluster Members	Binding Affinity (ΔG)	Dissociation Score at 37 °C (Kd)	Complex No.	Lowest Energy	Cluster Members	Binding Affinity (ΔG)	Dissociation Score at 37 °C (Kd)
Ephrin-B2 Host	HUMAN	1	−745.9	96	−11.8	5.00E-09	27	−713.3	131	−10.7	2.90E-08
	BAT	2	−753.7	29	−14.3	8.20E-11	28	−722.8	59	−12	3.30E-09
	CATTLE	3	−814.6	115	−12	3.20E-09	29	−735.6	100	−10.1	7.30E-08
	BUFFALO	4	−814.6	115	−12	3.20E-09	30	−735.6	100	−10.1	7.30E-08
	DOG	5	−814.6	115	−12	3.20E-09	31	−735.6	100	−10.1	7.30E-08
	GOAT	6	−814.6	115	−12	3.20E-09	32	−735.6	100	−10.1	7.30E-08
	DONKEY	7	−814.6	115	−12	3.20E-09	33	−735.6	100	−10.1	7.30E-08
	HORSE	8	−814.6	115	−12	3.20E-09	34	−735.6	100	−10.1	7.30E-08
	SHEEP	9	−814.6	115	−12	3.20E-09	35	−735.6	100	−10.1	7.30E-08
	PIG	10	−814.6	115	−12	3.20E-09	36	−735.6	100	−10.1	7.30E-08
	CAT	11	−812.6	113	−12.2	2.50E-09	37	−737.5	174	−11.5	7.60E-09
	MOUSE	12	−780.9	40	−12.2	2.50E-09	38	−700.6	72	−8	2.50E-06
	RAT	13	−773.7	33	−14	1.20E-10	39	−703	18	−15.8	7.10E-12
Ephrin-B3 Host	HUMAN	14	−1124.7	106	−19.1	3.40E-14	40	−1063.6	267	−12	3.70E-09
	BAT	15	−1124.7	106	−19.1	3.40E-14	41	−1063.6	267	−12	3.70E-09
	CATTLE	16	−1124.7	106	−19.1	3.40E-14	42	−1063.6	267	−12	3.70E-09
	BUFFALO	17	−1124.7	106	−19.1	3.40E-14	43	−1063.6	267	−12	3.70E-09
	DOG	18	−1124.7	106	−19.1	3.40E-14	44	−1063.6	267	−12	3.70E-09
	GOAT	19	−1124.7	106	−19.1	3.40E-14	45	−1063.6	267	−12	3.70E-09
	DONKEY	20	−1130.4	108	−18.4	9.80E-14	46	−1063.6	267	−12	3.70E-09
	HORSE	21	−1124.7	106	−19.1	3.40E-14	47	−1063.6	267	−12	3.70E-09
	SHEEP	22	−1124.7	106	−19.1	3.40E-14	48	−1063.6	267	−12	3.70E-09
	PIG	23	−1124.7	106	−19.1	3.40E-14	49	−1063.6	267	−12	3.70E-09
	CAT	24	−1118	100	−19	4.20E-14	50	−1089.9	276	−12.3	2.10E-09
	MOUSE	25	−1111.5	113	−18.6	8.30E-14	51	−1054	275	−12.6	1.20E-09
	RAT	26	−1111.5	113	−18.6	8.30E-14	52	−1054	275	−12.6	1.20E-09

was 3.30E-09 (at 37 °C).

3.4. Characterization of protein-protein interface

The PRODIGY webserver predicted the binding of study complexes according to contact-based interface interactions. The protein-protein interface residues that are involved in interchain interactions are highlighted in the multiple sequence alignment of Ephrin-B2 and B3 (Fig. 4). Analysis of the protein-protein interface helped better understand the trend in binding affinity scores of study complexes (Fig. 3 and Table 2). In NiV-B complexes with Ephrin-B2 (complexes 1 to 13), common interface residues were found between bat (ΔG −14.3 kcal/mol) and rat (ΔG −14 kcal/mol) which is consistent with their higher binding affinities compared to other species. In NiV-M complexes with

Ephrin-B2 (complexes 27 to 39), the highest binding affinity was found with rat (ΔG −15.8 kcal/mol) and the interface analysis reveals they had the greatest number of binding residues in the group. Major binding residues, like Pro95-Thr103 and Leu109-Phe113, outside the G-H loop were found in the interface between NiV-B complexes with Ephrin-B3 (complexes 14 to 26), this suggests why their binding affinities were strongest (ΔG −18.4 to −19.1 kcal/mol) among all four protein-protein complex groups. In NiV-M complexes with Ephrin-B3 (complexes 40 to 52), the binding energy scores of all study species were overlapping (ΔG −12 to −12.6 kcal/mol) since their interface residues were mostly identical. The contribution of different Ephrin-B2/B3 amino acids in binding varies in terms of the non-covalent bonds they form with NiV G and any inconsistencies between binding energy values may be due to other physicochemical properties of the interacting proteins.

4. Discussion

In this study, we assessed the extent to which different domestic and peridomestic mammals may serve as intermediate hosts for NiV infections based on *in silico* protein-protein interaction analysis of homology docked complexes between NiV G and host cell receptors Ephrin-B2 and B3. Overall, we found strong molecular evidence of potentially stable interactions in protein-protein complexes (n = 52) of NiV G with Ephrin-B2 and B3 of the study species. NiV-B strain is naturally more pathogenic than NiV-M strain, and NiV-B displayed stronger binding to both Ephrin-B2 and B3 in this study (Soman Pillai et al., 2020; Mire et al., 2016). No evidence of NiV infections in rats has been reported to date, but our analyses show that rat complexes had a high binding affinity compared to the known hosts and reservoirs of NiV.

Ephrin-B2 and B3 cell surface proteins exhibit a high degree of conservation across species, promoting NiV host tropism diversity (Xu et al., 2012).In this study, we found protein sequence homology (up to 100%) and close phylogenetic relationships between our study species' Ephrin-B2 and B3 proteins (Table 1 and Fig. 1). Ephrin-B receptor homology is a good indicator of host susceptibility if not a perfect one, as it does not necessarily indicate NiV permissibility or full viral replication in cells which is required for pathogenesis (Yoneda et al., 2006). Ephrin-B2 is expressed in vertebrates' venous and arterial endothelial cells, whereas in the central nervous system, both Ephrin-B2 and B3 are expressed (Negrete et al., 2006). NiV infection typically begins at the airway epithelium where Ephrin-B2 primarily binds to NiV G as its expression in respiratory tissues is higher than Ephrin-B3 (Negrete et al., 2006; Wong et al., 2002). In the later stages of infection, NiV G uses both Ephrin-B2 and B3 for cell attachment, especially in the central nervous system where they are co-expressed in varying patterns (Negrete et al., 2006). Our results show that Ephrin-B3 interactions with NiV G are strong, especially with the NiV-B strain. This explains the ability of NiV-B strain to produce severe neurological symptoms with long-term complications requiring more time for recovery since it possesses a higher affinity for Ephrin-B3 which is found in brain tissues (WHO, 2018; Mire et al., 2016).

Ephrin-B2 and B3 receptors share the same NiV G binding interface (Fig. 4). Previously reported Ephrin-B2 and B3 binding (G-H) loop residues Glu119-Trp125 critical for NiV G binding were detected in this study (Xu et al., 2008; Bowden et al., 2008a). We found that the Asn123-Trp125 binding interface residues in the G-H loop were conserved without any mutations in both Ephrin-B2 and B3 proteins. The Asn123-Trp125 residues bind with the highly hydrophobic surface of NiV G with van der Waals forces (Bowden et al., 2008a; Negrete et al., 2006). The binding affinity between the two proteins is typically affected by non-covalent intermolecular interactions, including hydrogen bonding, electrostatic interactions, hydrophobic interactions, and Van der Waals forces. In addition, the binding affinity between NiV G and Ephrin-B2/B3 *in vivo* may be influenced by the other molecules present in the body. The relatively lower binding affinity of NiV-G for Ephrin-B2 compared to B3 in this study opposes previously reported kinetics data. Ephrin-B2 has a slower off-rate and takes longer time to detach from NiV-G resulting in slightly higher affinity (Negrete et al., 2006). These findings probably differ due to the nature of the data since molecular docking analyses the most energetically favourable pose, assuming the lowest energy pose represents the most likely binding mode, whereas kinetics data is derived from experimentally measuring the real-time interaction between molecules (Kozakov et al., 2017; Negrete et al., 2006). Differences in Kd values of the predicted protein-protein interaction of the study complexes with NiV-B and NiV-M may arise due to factors such as molecule concentration, stoichiometry,

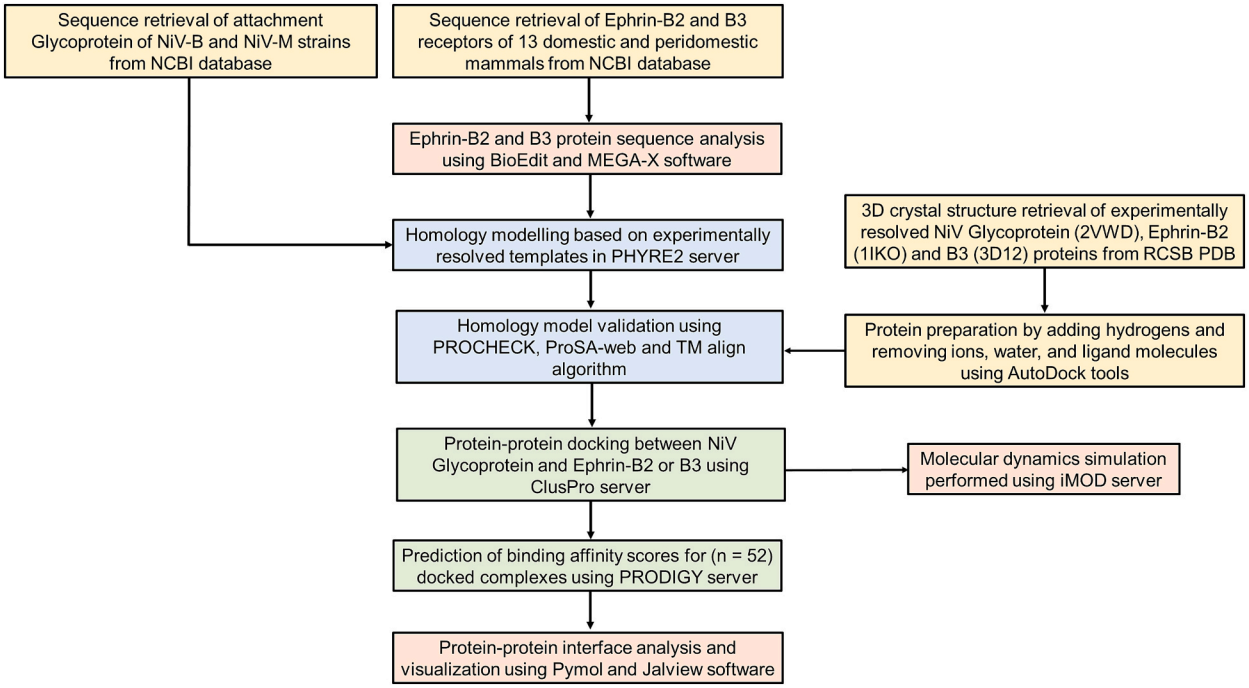

Fig. 1. Schematic presentation of the overall workflow for *in silico* prediction of NiV host tropism in this study.

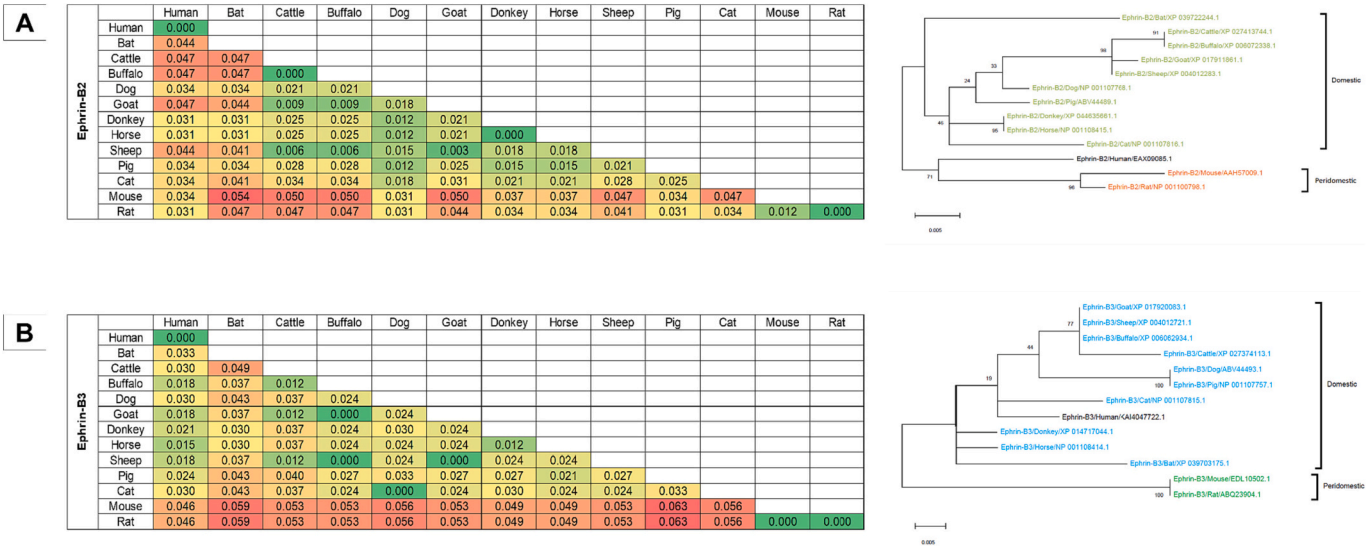

A

Ephrin-B2

	Human	Bat	Cattle	Buffalo	Dog	Goat	Donkey	Horse	Sheep	Pig	Cat	Mouse	Rat
Human	0.000												
Bat	0.044												
Cattle	0.047	0.047											
Buffalo	0.047	0.047	0.000										
Dog	0.034	0.034	0.021	0.021									
Goat	0.047	0.044	0.009	0.009	0.018								
Donkey	0.031	0.031	0.025	0.025	0.012	0.021							
Horse	0.031	0.031	0.025	0.025	0.012	0.021	0.000						
Sheep	0.044	0.041	0.006	0.006	0.015	0.003	0.018	0.018					
Pig	0.034	0.034	0.028	0.028	0.012	0.025	0.015	0.015	0.021				
Cat	0.034	0.041	0.034	0.034	0.018	0.031	0.021	0.021	0.028	0.025			
Mouse	0.034	0.054	0.050	0.050	0.031	0.050	0.037	0.037	0.047	0.034	0.047		
Rat	0.031	0.047	0.047	0.047	0.031	0.044	0.034	0.034	0.041	0.031	0.034	0.012	0.000

B

Ephrin-B3

	Human	Bat	Cattle	Buffalo	Dog	Goat	Donkey	Horse	Sheep	Pig	Cat	Mouse	Rat
Human	0.000												
Bat	0.033												
Cattle	0.030	0.049											
Buffalo	0.018	0.037	0.012										
Dog	0.030	0.043	0.037	0.024									
Goat	0.018	0.037	0.012	0.000	0.024								
Donkey	0.021	0.030	0.037	0.024	0.030	0.024							
Horse	0.015	0.030	0.037	0.024	0.024	0.024	0.012						
Sheep	0.018	0.037	0.012	0.000	0.024	0.000	0.024	0.024					
Pig	0.024	0.043	0.040	0.027	0.033	0.027	0.027	0.021	0.027				
Cat	0.030	0.043	0.037	0.024	0.000	0.024	0.030	0.024	0.024	0.033			
Mouse	0.046	0.059	0.053	0.053	0.056	0.053	0.049	0.049	0.053	0.063	0.056		
Rat	0.046	0.059	0.053	0.053	0.056	0.053	0.049	0.049	0.053	0.063	0.056	0.000	0.000

Fig. 2. Protein sequence analysis of (A) Ephrin-B2 and (B) Ephrin-B3 receptors from domestic and peridomestic mammals. The dissimilarity in protein sequence among Ephrin-B2 and B3 of the study species is shown in the *p*-distance matrix. The phylogenetic tree was constructed with 1000 bootstrap replications through the Maximum Likelihood method and JTT matrix-based model, and evolutionary distances were computed using the JTT model. The scale bar in the phylogenetic tree denotes the length of 0.5% amino acid sequence variance or genetic distances.

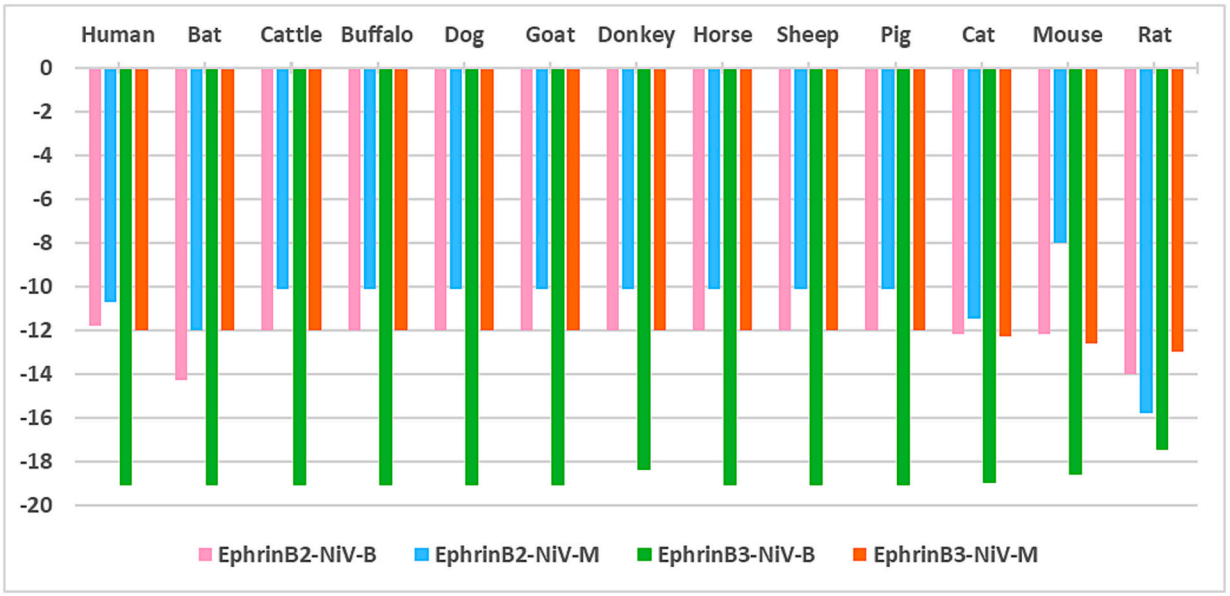

Fig. 3. Distribution of binding affinity ΔG (kcal/mol) scores of NiV G complexes with Ephrin-B2 and Ephrin-B3 of domestic and peridomestic mammals calculated using the PRODIGY web server.

allostery, and other conditions that can shift the equilibrium between bound and unbound states, leading to changes in Kd without affecting the binding affinity (Kastritis et al., 2011). Further limitations that may cause *in silico* data to deviate from the true binding affinity values include bias to protein template structures (Vakser, 2014). The lack of available experimentally derived structure data may lead to poor or fragmentary template selection, which subsequently produces inaccuracies in the template-model alignment and positioning of side chains or loops in homology models (Vakser, 2014). Our model validation scores indicate high credibility of the homology model design and selection done in this study. We employed the double-homology method which further increases the challenges of accurately predicting the binding strength for any given protein-protein complex. However, both Cluspro and PRODIGY are highly effective tools that accurately predict the interactions of double-homology docked complexes (Kozakov et al., 2017; Xue et al., 2016).

There is an epidemiological link between human NiV infections and close contact with sick or dead ruminants (Paton et al., 1999). Serological evidence of NiV infections in animals is limited to the detection of non-neutralizing antibodies against NiV G in different countries (Chowdhury et al., 2014; Kasloff et al., 2019; Hayman et al., 2011). However, the presence of non-neutralizing antibodies may result from cross-reactivity with other NiV-like viruses and it does not indicate natural NiV transmission or infection in animals (Chowdhury et al., 2014; Kasloff et al., 2019; Hayman et al., 2011). In Bangladesh, most of human NiV infections arise from consuming date palm sap contaminated with *Pteropus* excreta or through person-to-person transmission (Nikolay et al., 2019; Luby et al., 2006). Implementing large-scale behavioural and cultural changes in the NiV outbreak areas in Bangladesh can help prevent infections in the human population (Nahar et al., 2017). The

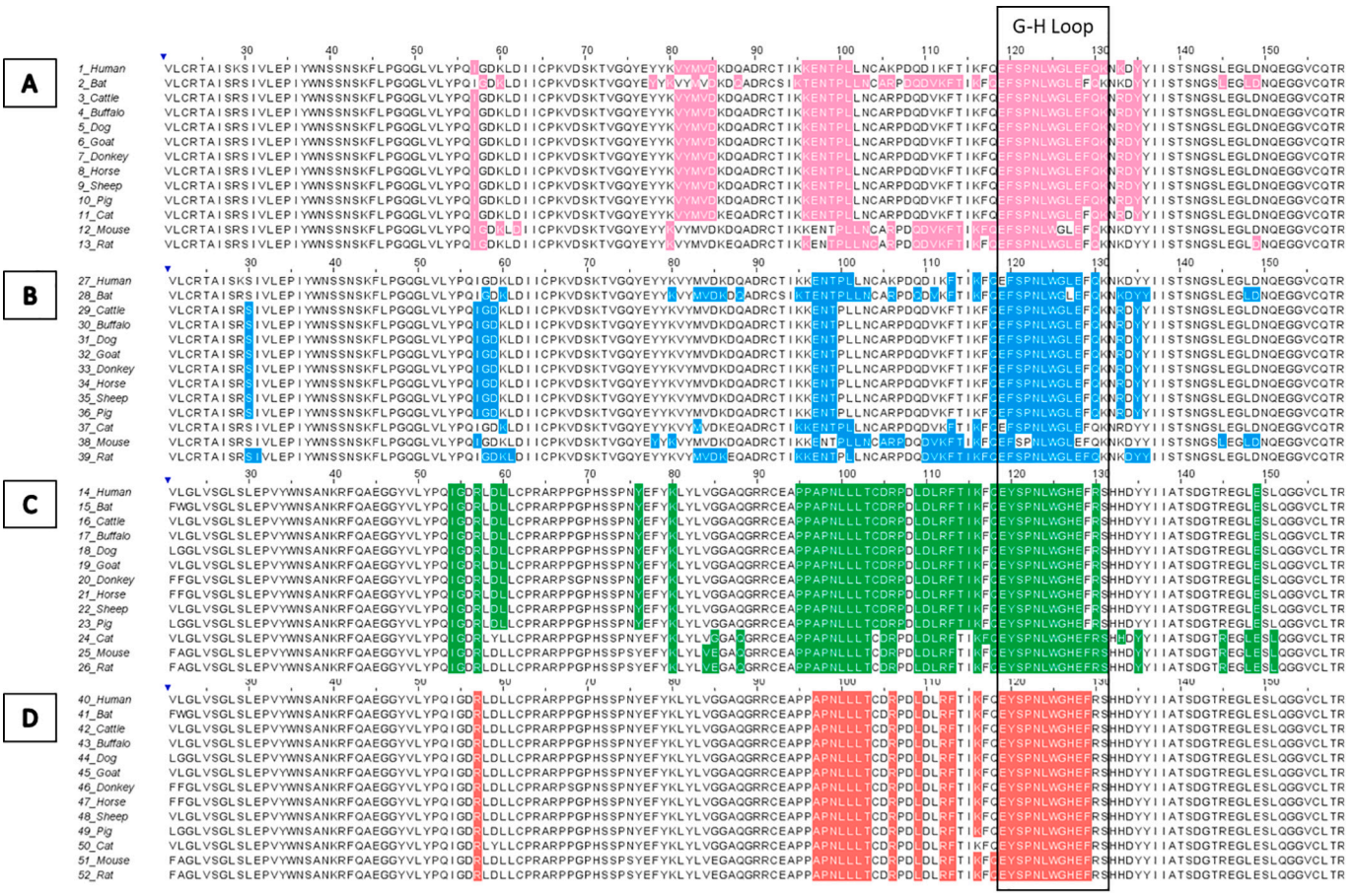

Fig. 4. Amino acid alignment of Ephrin-B2 and Ephrin-B3 protein sequence from different species. Name of domestic or peridomestic animals and their corresponding docking complex ($n = 52$) numbers are listed on the left. Coloured sequences indicate amino acid residues involved in interactions at the protein-protein interface of (A) NiV-B with Ephrin-B2, (B) NiV-M with Ephrin-B2, (C) NiV-B with Ephrin-B3 and (D) NiV-M with Ephrin-B3 docking complexes.

probable transmission routes in animals, like their feeding habits, are expected to be different from humans. Although in many areas, spoiled date palm sap is fed to livestock as the high sugar content makes it an easy energy source (Chowdhury et al., 2014). Therefore, continuous examination of animals reared around *Pteropus* bat roosts in NiV endemic areas is required.

Understanding the dynamics of NiV in potentially susceptible peridomestic animal populations will help comprehend the shared risk for the future and enhance the efforts for drug or vaccine development. Apart from the immediate risks NiV infections in domestic and peridomestic animals pose to humans, it may facilitate the evolutionary adaptation of NiV to mammals beyond bats. There are diverse strains of NiV circulating in fruit bats of the *Pteropodidae* family due to selective pressures like ecological and immunological characteristics of bats (Whitmer et al., 2020; Epstein et al., 2020). The broad geographic range of bats allows spill over to humans and other animals (Epstein et al., 2020). We should also consider reverse zoonosis of NiV as already seen with severe acute respiratory syndrome coronavirus 2 (SARS-CoV-2) infections in animals like rats during the coronavirus disease of 2019 (COVID-19) pandemic (Glud et al., 2021; Miot et al., 2022). NiV has not been found in rats till now, but our analysis identifies the rat (*R. norvegicus*) as a peridomestic animal of concern requiring special research attention (Drexler et al., 2012). Although susceptibility has been predicted *in silico*, further investigation is required to gain a deeper knowledge of NiV host or intermediate host competence in *Rattus*, especially in the context of Bangladesh where species diversity is high.

5. Conclusion

We explored the susceptibility of various domestic and peridomestic mammalian hosts to NiV infection to identify potential intermediate hosts that pose risks to the human population. Our results show that NiV G can form stable interactions with Ephrin-B2 and B3 receptors in several domestic and peridomestic mammalian species which could increase the possibility of further potential large-scale outbreaks. Rats (*R. norvegicus*) should be investigated as possible wildlife reservoirs of NiV due to their relatively high susceptibility to NiV infection. However, more research is necessary to address a number of concerns regarding NiV infections in rats and their role in NiV transmission to humans. To conclude, our findings will have significant implications for improving our understanding of NiV epidemiology and pathogenesis in both humans and animals, as well as for the development of novel therapeutics.

Funding

The core donors of icddr,b provided support for this research work.

CRediT authorship contribution statement

Ananya Ferdous Hoque: Conceptualization, Methodology, Software, Validation, Formal analysis, Visualization, Writing – original draft. **Md. Mahfuzur Rahman:** Conceptualization, Formal analysis, Methodology, Software, Validation, Writing - original draft. **Ayeasha Siddika Lamia:** Methodology, Software, Validation, Visualization.

Ariful Islam: Writing – review & editing. **John D. Klena:** Writing – review & editing. **Syed Moinuddin Satter:** Writing – review & editing. **Joel M. Montgomery:** Writing – review & editing. **Mohammad Enayet Hossain:** Writing – review & editing. **Tahmina Shirin:** Writing – review & editing. **Iqbal Kabir Jahid:** Writing – review & editing. **Mohammed Ziaur Rahman:** Conceptualization, Writing – review & editing, Supervision, Funding acquisition.

Declaration of Competing Interest

The authors confirm the absence of any conflicts of interest. The findings and conclusions presented in this report are solely those of the authors and do not necessarily reflect the official stance of the Centers for Disease Control and Prevention.

Data availability

The datasets generated or analysed during this study are included in this article and its supplementary information files.

Acknowledgements

The research study received funding from the core donors who support icddr,b's operations and research. Presently, the Governments of Bangladesh, Canada, Sweden, and the UK are among the donors providing unrestricted support. We express our sincere gratitude to our core donors for their support and dedication to icddr,b's research endeavours.

Appendix A. Supplementary data

Supplementary data to this article can be found online at https://doi.org/10.1016/j.meegid.2023.105516.

References

Aditi, Shariff, M., 2019. Nipah Virus Infection: A Review, 147, p. e95.
Banerjee, S., et al., 2019. Nipah virus disease: a rare and intractable disease. Intractab. & Rare Diseas. Res. 8 (1), 1–8.
Bellini, W.J., et al., 2005. Nipah virus: an emergent paramyxovirus causing severe encephalitis in humans. J. Neuro-Oncol. 11 (5), 481–487.
Berman, H.M., et al., 2000. The Protein Data Bank. Nucleic Acids Res. 28 (1), 235–242.
Bhuiyan, M.A., et al., 2022. Discovery of Potential Compounds against Nipah Virus: A Molecular Docking and Dynamics Simulation Approaches. Research Square.
Biosafety in Microbiological and Biomedical Laboratories (BMBL) 6th Edition, 2020. Centers for Disease Control and Prevention (CDC) and National Institutes of Health (NIH).
Bioterrorism Agents/Diseases, 2023. Centers for Disease Control and Prevention.
Bossart, K.N., et al., 2007. Functional studies of host-specific ephrin-B ligands as Henipavirus receptors. Virology 372 (2), 357–371.
Bowden, T.A., et al., 2008a. Structural basis of Nipah and Hendra virus attachment to their cell-surface receptor ephrin-B2. Nat. Struct. Mol. Biol. 15 (6), 567–572.
Bowden, T.A., et al., 2008b. Crystal structure and carbohydrate analysis of Nipah virus attachment glycoprotein: a template for antiviral and vaccine design. J. Virol. 82 (23), 11628–11636.
Cheliout Da Silva, S., Yan, L., Dang, H.V., 2021. Functional analysis of the fusion and attachment glycoproteins of mojiang henipavirus, 13 (3).
Chowdhury, S., et al., 2014. Serological evidence of Henipavirus exposure in cattle, goats and pigs in Bangladesh. PLoS Negl. Trop. Dis. 8 (11), e3302.
Clayton, B.A., et al., 2012. Transmission routes for nipah virus from Malaysia and Bangladesh. Emerg. Infect. Dis. 18 (12), 1983–1993.
de Wit, E., Munster, V.J., 2015. Animal models of disease shed light on Nipah virus pathogenesis and transmission. J. Pathol. 235 (2), 196–205.
Drexler, J.F., et al., 2012. Bats host major mammalian paramyxoviruses. Nat. Commun. 3, 796.
Epstein, J.H., et al., 2020. Nipah virus dynamics in bats and implications for spillover to humans. Proc. Natl. Acad. Sci. 117 (46), 29190–29201.
Glud, H.A., et al., 2021. Zoonotic and reverse zoonotic transmission of viruses between humans and pigs. Apmis 129 (12), 675–693.
Harcourt, B.H., et al., 2005. Genetic characterization of Nipah virus, Bangladesh, 2004. Emerg. Infect. Dis. 11 (10), 1594–1597.
Hauser, N., et al., 2021. Evolution of nipah virus infection: past, present, and future considerations, 6 (1).
Hayman, D.T., et al., 2011. Antibodies to henipavirus or henipa-like viruses in domestic pigs in Ghana, West Africa. PLoS One 6 (9), e25256.
Kasloff, S.B., et al., 2019. Pathogenicity of Nipah henipavirus Bangladesh in a swine host. Sci. Rep. 9 (1), 5230.
Kastritis, P.L., et al., 2011. A structure-based benchmark for protein-protein binding affinity. Protein Sci. 20 (3), 482–491.
Kelley, L.A., et al., 2015. The Phyre2 web portal for protein modeling, prediction and analysis. Nat. Protoc. 10 (6), 845–858.
Kozakov, D., et al., 2017. The ClusPro web server for protein–protein docking. Nat. Protoc. 12 (2), 255–278.
Luby, S.P., et al., 2006. Foodborne transmission of Nipah virus, Bangladesh. Emerg. Infect. Dis. 12 (12), 1888.
Mills, J.N., et al., 2009. Nipah virus infection in dogs, Malaysia, 1999. Emerg. Infect. Dis. 15 (6), 950–952.
Miot, E.F., et al., 2022. Surveillance of rodent pests for SARS-CoV-2 and other coronaviruses. Hong Kong. Emerg. Infect. Dis. 28 (2), 467–470.
Mire, C.E., et al., 2016. Pathogenic differences between Nipah virus Bangladesh and Malaysia strains in Primates: implications for antibody therapy. Sci. Rep. 6, 30916.
Mlikovsky, J., 2012. Correct name for the Indian flying fox (Pteropodidae). Vespertilio 16, 203–210.
Nahar, N., et al., 2017. A large-scale behavior change intervention to prevent Nipah transmission in Bangladesh: components and costs. BMC. Res. Notes 10 (1), 225.
Negrete, O.A., et al., 2006. Two key residues in ephrinB3 are critical for its use as an alternative receptor for Nipah virus. PLoS Pathog. 2 (2), e7.
Nikolay, B., et al., 2019. Transmission of Nipah virus—14 years of investigations in Bangladesh. N. Engl. J. Med. 380 (19), 1804–1814.
Outbreak of Hendra-like virus–Malaysia and Singapore, 1998–-1999, 1999. MMWR Morb. Mortal. Wkly Rep, 48(13), pp. 265–269.
Paton, N.I., et al., 1999. Outbreak of Nipah-virus infection among abattoir workers in Singapore. Lancet 354 (9186), 1253–1256.
Skowron, K., et al., 2022. Nipah Virus–Another Threat From the World of Zoonotic Viruses. Front. Microbiol. 12.
Soman Pillai, V., Krishna, G., Valiya Veettil, M., 2020. Nipah virus: past outbreaks and future containment. Viruses 12 (4), 465.
Toth, J., et al., 2001. Crystal structure of an ephrin ectodomain. Dev. Cell 1 (1), 83–92.
Vakser, I.A., 2014. Protein-protein docking: from interaction to interactome. Biophys. J. 107 (8), 1785–1793.
Wang, Z., et al., 2022. Architecture and antigenicity of the Nipah virus attachment glycoprotein. Science 375 (6587), 1373–1378.
Waterhouse, A.M., et al., 2009. Jalview version 2—a multiple sequence alignment editor and analysis workbench. Bioinformatics 25 (9), 1189–1191.
Weingartl, H.M., Berhane, Y., Czub, M., 2009. Animal models of henipavirus infection: a review. Vet. J. 181 (3), 211–220.
Whelan, S., Goldman, N., 2001. A general empirical model of protein evolution derived from multiple protein families using a maximum-likelihood approach. Mol. Biol. Evol. 18 (5), 691–699.
Whitmer, S.L.M., et al., 2020. Inference of Nipah virus evolution, 1999–2015. Virus Evolut. 7 (1).
WHO, 2018. Nipah Virus. Fact Sheets. Available from: https://www.who.int/news-room/fact-sheets/detail/nipah-virus.
WHO, 2018. Prioritizing Diseases for Research and Development in Emergency Contexts. The WHO R&D Blueprint Team.
Wiederstein, M., Sippl, M.J., 2007. ProSA-web: interactive web service for the recognition of errors in three-dimensional structures of proteins. Nucleic Acids Res. 35 (Web Server issue), W407–W410.
Wong, K.T., et al., 2002. Nipah virus infection: pathology and pathogenesis of an emerging Paramyxoviral zoonosis. Am. J. Pathol. 161 (6), 2153–2167.
Wong, K.T., et al., 2003. A golden hamster model for human acute Nipah virus infection. Am. J. Pathol. 163 (5), 2127–2137.
Wu, Z., et al., 2014. Novel Henipa-like virus, Mojiang Paramyxovirus, in rats, China, 2012. Emerg. Infect. Dis. 20 (6), 1064–1066.
Xu, K., et al., 2008. Host cell recognition by the henipaviruses: crystal structures of the Nipah G attachment glycoprotein and its complex with ephrin-B3. Proc. Natl. Acad. Sci. U. S. A. 105 (29), 9953–9958.
Xu, K., Broder, C.C., Nikolov, D.B., 2012. Ephrin-B2 and ephrin-B3 as functional henipavirus receptors. Semin. Cell Dev. Biol. 23 (1), 116–123.
Xue, L.C., et al., 2016. PRODIGY: a web server for predicting the binding affinity of protein–protein complexes. Bioinformatics 32 (23), 3676–3678.
Yoneda, M., et al., 2006. Establishment of a Nipah virus rescue system. Proc. Natl. Acad. Sci. 103 (44), 16508–16513.
Zhang, Y., Skolnick, J., 2005. TM-align: a protein structure alignment algorithm based on the TM-score. Nucleic Acids Res. 33 (7), 2302–2309.